Stepwise photoinduced electron transfer in a tetrathiafulvalene-phenothiazine-ruthenium triad

Michael Skaisgirski, Christopher B. Larsen, Christoph Kerzig, and Oliver S. Wenger*

Abstract: A molecular triad comprised of a $[Ru(bpy)_3]^{2+}$ (bpy = 2,2'-bipyridine) photosensitizer, a primary phenothiazine (PTZ) donor and a secondary (extended) tetrathiafulvalene (exTTF) donor was synthesized and explored by UV-Vis transient absorption spectroscopy. Initial photoinduced electron transfer from PTZ to the ^{3}MLCT-excited $[Ru(bpy)_3]^{2+}$ occurs within less than 60 ps, and subsequently PTZ is regenerated by electron transfer from exTTF with a time constant of 300 ps. The resulting photoproduct comprised of $exTTF^{\bullet+}$ and $[Ru(bpy)_3]^{+}$ has a lifetime of 6100 ps in de-aerated CH_3CN at room temperature. Additional one- and two-pulse laser flash photolysis studies of the triad were performed in the presence of excess methyl viologen (MV^{2+}), to explore the possibility of light-driven charge accumulation on exTTF. MV^{2+} clearly oxidized $[Ru(bpy)_3]^{+}$ and thereby re-instated ground-state $[Ru(bpy)_3]^{2+}$ in triads in which exTTF had been oxidized to $exTTF^{\bullet+}$, but further excitation of the solution containing the $exTTF^{\bullet+}$-PTZ-$[Ru(bpy)_3]^{2+}$ photoproduct did not provide evidence for $exTTF^{2+}$. Nevertheless, it seems that the design principle of a covalent donor-donor-sensitizer triad (as opposed to simpler donor-sensitizer dyads) is beneficial for light-driven accumulation of oxidation equivalents. These investigations are relevant in the greater context of multi-electron photoredox chemistry and artificial photosynthesis.

Introduction

The photoinduced transfer of single electrons in donor-acceptor compounds has been thoroughly investigated for several decades, but light-driven multi-electron transfer processes are still very poorly understood. For small-molecule activation and artificial photosynthesis multi-electron transfer is essential, and therefore it is highly desirable to understand the basic principles of this reaction type.[1] Fully integrated molecular systems comprised of covalently connected donors, sensitizers, and acceptors are ideally suited for mechanistic studies with time-resolved laser spectroscopy. In most cases explored to date, light-induced charge accumulation relies on sacrificial reagents that decompose after electron transfer,[2] but this does not permit sustainable light-to-chemical energy conversion. However, in absence of sacrificial reagents all photoinduced electron transfer steps are reversible, and this commonly leads to a multitude of undesired reverse electron transfers which are counter-productive, making charge accumulation very difficult.[1, 3] Two pioneering studies reported on light-driven charge accumulation in molecular systems without sacrificial reagents more than 20 years ago,[4] but the field had then been dormant until 2010 when TiO_2 nanoparticles were used to facilitate accumulation of oxidative equivalents on covalently attached donors.[5] More recently, we and others reported on several fully integrated donor-sensitizer-acceptor compounds that permitted long-lived (> 10 ns) charge accumulation in the absence of sacrificial reagents,[6] sometimes exploiting proton-coupled electron transfer (PCET),[7] or the concept of redox potential inversion.[8]

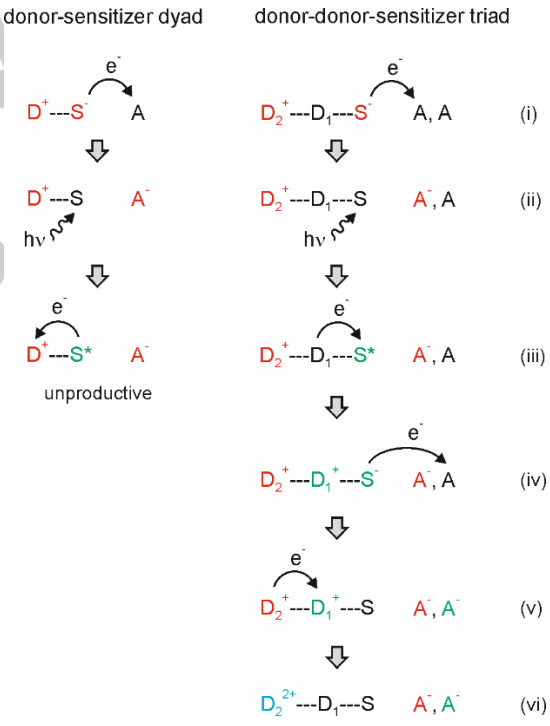

Scheme 1. Possible reaction pathways after primary charge-separation and excitation with a second photon in simple donor-sensitizer (D-S) dyads (left) and in donor-donor-sensitizer triads (right).

Primary electron-hole separation after excitation with a first photon is usually facile, but the processes occurring after the absorption of a second photon are often complicated, as illustrated by Scheme 1. In simple donor-sensitizer (D-S) compounds (left part), primary photoinduced electron transfer yields D^+-S^-, and the latter can donate its additional electron to

[*] Dr. M. Skaisgirski, Dr. C. B. Larsen, Dr. C. Kerzig, Prof. Dr. O. S. Wenger
Department of Chemistry, University of Basel
St. Johanns-Ring 19, 4056 Basel, Switzerland
E-mail: oliver.wenger@unibas.ch

Supporting information for this article is given via a link at the end of the document.

free acceptors (A) in a bimolecular reaction. When the resulting D^+-S intermediate is excited with a second photon (line ii), then the fastest reaction is usually oxidative quenching of the excited sensitizer, because D^+ is a strong acceptor. This step is unproductive for charge accumulation because it occurs in the wrong direction. In the present study we aimed to explore whether this fundamental problem can be overcome in donor-donor-sensitizer (D_2-D_1-S) compounds.

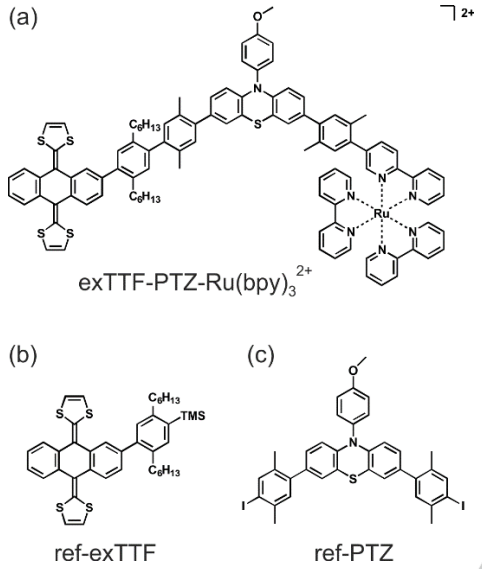

Scheme 2. Molecular structures of the triad under study (a) and two reference compounds (b, c).

When D_2 is the stronger donor than D_1, then initial excitation of S will lead to D_2^+-D_1-S^- (right part of Scheme 1, line i) in a sequence of electron transfer steps that will be studied in detail below. After electron transfer from S^- to a first acceptor molecule (A) and subsequent secondary excitation of S (line ii), electron transfer from D_1 to S* could now outcompete the more exergonic electron transfer from S* to D_2^+ because of the shorter distance associated with the desirable reductive quenching of S* by D_1 (line iii). After bimolecular electron transfer between S^- and a second acceptor molecule (A) (line iv) and intramolecular charge-shift between D_2^+ and D_1^+ (line v), hole accumulation on D_2 will have occurred (line vi).

Successful realization of this concept requires a primary donor (D_1) that can reductively quench the excited sensitizer, and a stronger secondary donor (D_2) that can be oxidized twice. Moreover, the one-electron oxidized form of the secondary two-electron donor (D_2^+) must be thermodynamically able to reduce the one-electron oxidized form of the primary donor (D_1^+). Ideally, all relevant intermediates and photoproducts (S*, S^-, D_1^+, D_2^+, D_2^{2+}, A^-) should have diagnostic spectral signatures that can easily be detected by transient absorption spectroscopy, and mutual spectral overlaps should be minimal. These combined factors represent a very stringent set of selection criteria for the individual components of suitable D_2-D_1-S triads. Based on previously published electrochemical and spectroscopic data, we identified the combination of a phenothiazine (PTZ) primary donor (D_1) with an extended tetrathiafulvalene (exTTF) unit as a secondary two-electron donor (D_2), and a $Ru(bpy)_3^{2+}$ sensitizer (S) as a promising molecular design (Scheme 2a).

There have been several prior studies of photoinduced electron and energy transfer in which either TTF-Ru^{II} dyads,[9] or PTZ-Ru^{II} compounds have been explored,[10] but never in a combined triad system such as that in Scheme 2a. To the best of our knowledge, there are no prior published reports that tested the concept outlined in Scheme 1. Furthermore, we are unaware of previous papers reporting the light-driven charge accumulation on exTTF, and it seems that merely one-electron oxidation of exTTF has been achievable in photoinduced manner until now.[11] However, pulse radiolysis studies provided evidence for disproportionation of $exTTF^{\bullet+}$ into $exTTF^{2+}$ and exTTF.[12] The redox chemistry of so-called π-extended versions of TTF has received considerable attention,[13] and exTTF has been incorporated into a variety of supramolecular constructs relevant in the greater context of molecular electronics.[14]

Table 1. Redox potentials (E^0 in V vs SCE) of the individual components of the triad, the two reference compounds, and the photosensitizer.

redox couple	**exTTF-PTZ-$Ru(bpy)_3^{2+}$** [a]	**ref-exTTF** [b]	**ref-PTZ** [b]	$Ru(bpy)_3^{2+}$ [c]
$exTTF^{\bullet+/0}$	0.42	0.43		
$exTTF^{2+/\bullet+}$	0.05	0.10		
$PTZ^{\bullet+/0}$	0.68		0.75	
$Ru(bpy)_3^{3+/2+}$	1.29			1.29
$Ru(bpy)_3^{2+/+}$				-1.33

[a] In CH_3CN. [b] In DMF. [c] From ref. [15].

Results and Discussion

The **exTTF-PTZ-$Ru(bpy)_3^{2+}$** triad in Scheme 2a was synthesized from commercial building blocks as described in detail in the Supporting Information (SI, pages S1-S7). The final product was characterized by NMR spectroscopy, high-resolution mass spectrometry, and combustion analysis (SI, page S7). The multi-step ligand synthesis (Scheme S1) involved the preparation and isolation of compounds **ref-exTTF** (Scheme 2b) and **ref-PTZ** (Scheme 2c), which served as convenient reference substances for electrochemical and optical spectroscopic investigations.

Cyclic voltammetry of the three compounds from Scheme 2 (Figure S1) was performed in de-aerated CH_3CN (triad) or DMF (reference substances) and provided the redox potentials in Table 1, which are all in line with previously reported potentials for related molecular components.[16] Based on the known redox potentials for $Ru(bpy)_3^{2+}$ and an energy of 2.12 eV for its photoactive ^{3}MLCT excited state, the reduction potential of the

excited sensitizer unit (S*) is ca. 0.8 V vs SCE. Thus, primary electron transfer from PTZ to ^{3}MLCT-excited $Ru(bpy)_3^{2+}$ is slightly exergonic ($\Delta G_{ET}^0 \approx$ - 0.05 eV), and charge-shift from exTTF to $PTZ^{\bullet+}$ has a reaction free energy of ca. -0.7 eV based on the potentials in Table 1. Furthermore, even the more challenging electron transfer from $exTTF^{\bullet+}$ to $PTZ^{\bullet+}$ (an anticipated necessary process in the course of possible charge accumulation; Scheme 1, right, line v) is exergonic by ca. 0.3 eV, hence the thermodynamic requirements for hole accumulation are fulfilled.

In the UV-Vis absorption spectrum of the **exTTF-PTZ-Ru(bpy)$_3^{2+}$** triad (Figure S2), the MLCT absorption bands of the sensitizer unit appear as a low-energy shoulder to more intense exTTF-localized π-π^* absorption bands. Nevertheless, selective excitation of the $Ru(bpy)_3^{2+}$ unit is readily possible, especially into the low-energy tail at 532 nm.

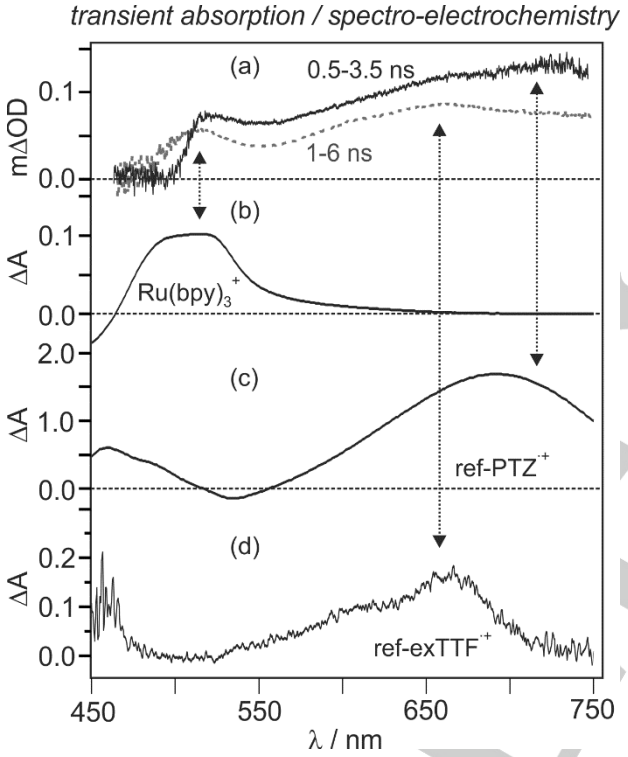

Figure 1. (a) Transient absorption spectra of the triad in de-aerated CH_3CN after excitation at 532 nm (see Experimental Section for details). Detection occurred by time-integration between 0.5 – 3.5 ns (black solid trace) and between 1 - 6 ns (gray dotted trace) following excitation with pulses of ca. 30 ps duration. (b) UV-Vis difference spectrum obtained as a result of reduction of $Ru(bpy)_3^{2+}$ to $Ru(bpy)_3^+$ in dry, de-oxygenated CH_3CN (with 0.1 M $TBAPF_6$) at a potential of -1.4 V vs SCE (see Figure S3). (c) UV-Vis difference spectrum obtained as a result of conversion of the PTZ moiety of the triad to $PTZ^{\bullet+}$ in dry CH_2Cl_2, using $SbCl_5$ as chemical oxidant (see Figure S5). (d) Difference spectrum resulting from photochemical oxidation of **ref-exTTF** to **ref-exTTF$^{\bullet+}$** in DMF (see Figure S4).

Picosecond transient absorption studies were performed on solutions of the triad in de-aerated CH_3CN at room temperature, using an excitation wavelength of 532 nm and a pulse duration of ca. 30 ps. Measurements with a streak camera (see Experimental Section for details) permitted simultaneous recording of temporally and spectrally resolved data. Time-integrating between 0.5 and 3.5 ns following excitation, a fundamentally different ΔOD spectrum was recorded than between 1 and 6 ns (black solid vs gray dotted traces in Figure 1a). Both spectra exhibit absorption bands at ca. 510 nm and 660 nm, but the early spectrum features an additional band near 700 nm not present in the 1 – 6 ns spectrum. Spectro-electrochemical experiments with $[Ru(bpy)_3](PF_6)_2$ (Figure 1b), **ref-PTZ** (Figure 1c), as well as a nanosecond flash-photolysis experiment that produced **ref-exTTF$^{\bullet+}$** (Figure 1d) were useful to assign the individual transient absorption bands in Figure 1a to different electron transfer products (dotted vertical arrows). Reduction of $Ru(bpy)_3^{2+}$ to $Ru(bpy)_3^+$ at -1.4 V vs SCE caused an increase in extinction at 510 nm (Figure 1b, Figure S3), in line with prior reports - hence the observable bands at that wavelength in Figure 1a are assigned to the one-electron reduced sensitizer.[17] In the transient absorption spectra in Figure 1a, a pronounced decrease of change in absorbance at wavelengths shorter than 520 nm (accompanied by decreased signal-to-noise ratio) can be observed, which does not follow the difference spectrum in Figure 1b. This is due to the high optical density of the sample used for the picosecond transient absorption measurements, precluding detection at wavelengths below 500 nm.

The band at 660 nm is attributed to the one-electron oxidized TTF donor based on the data in Figure 1d, in line with prior studies.[12] To obtain the difference spectrum in Figure 1d, a solution containing 30 μM $[Ru(bpy)_3](PF_6)_2$ and 2 mM **ref-exTTF** in de-aerated DMF was excited at 532 nm with laser pulses of ca. 10 ns duration (see SI page S10). Bimolecular electron transfer between **ref-exTTF** and photoexcited $Ru(bpy)_3^{2+}$ produced a difference spectrum with overlapping contributions from **ref-exTTF$^{\bullet+}$** and $Ru(bpy)_3^+$ (Figure S4a). Subtraction of the contribution of the latter (obtained via spectro-electrochemistry; Figure S3/S4b) yielded the difference spectrum shown in Figure 1d, which is very similar to previously reported spectra for one-electron oxidized exTTF.[12]

Lastly, the band observable near 700 nm in the 0.5 – 3.5 ns spectrum of Figure 1a can be attributed to $PTZ^{\bullet+}$ based on the spectro-electrochemical data in Figure 1c (see Figure S5 and SI page S10), and this difference spectrum is compatible with previously published $PTZ^{\bullet+}$ spectra.[10d, 18] At longer detection times (1 – 6 ns spectrum, gray dotted trace in Figure 1a), a shift in absorption band maximum closer to 660 nm suggests that $PTZ^{\bullet+}$ is a very short-lived intermediate whilst $exTTF^{\bullet+}$ is the longer-lived photoproduct.

This interpretation is corroborated by the transients shown in Figure 2. The black trace in (a) is the temporal evolution of the absorption signal integrated between 580 and 700 nm after excitation at 532 nm with laser pulses of ca. 30 ps duration. This corresponds to the spectral range in which both $PTZ^{\bullet+}$ and $exTTF^{\bullet+}$ absorb (Figure 1a/c/d). This signal exhibits an initial rapid increase that is instrumentally limited, followed by a rise with a time constant of ca. 300 ps. The initial rapid rise parallels the instrumentally limited evolution of the ^{3}MLCT absorption features of $[Ru(bpy)_3]^{2+}$ in a reference sample (gray trace in Figure 2b),[19] and a time-resolved emission experiment with the triad shows that

the ^{3}MLCT-excited state decays with instrumentally limited kinetics (Figure S6). Consequently, we attribute the initial rapid rise in the black trace of Figure 2a to primary electron transfer from PTZ to ^{3}MLCT-excited $Ru(bpy)_3^{2+}$ occurring with a time constant shorter than 60 ps (ET_1 in Scheme 3). In related systems, similarly rapid initial electron transfers were observed.[20] The slower rise (τ = 300 ps) can be attributed to secondary electron transfer from exTTF to $PTZ^{\bullet+}$ (ET_2 in Scheme 3), leading to the final **exTTF$^{\bullet+}$-PTZ-Ru(bpy)$_3^+$** photoproduct. Based on the redox potentials from Table 1, that photoproduct stores 1.76 eV of energy. Given the relatively large reorganization energy associated with oxidation of $TTF^{\bullet+}$ to TTF and the comparatively low driving-forces for ET_1 and ET_2,[21] these processes are quite rapid.

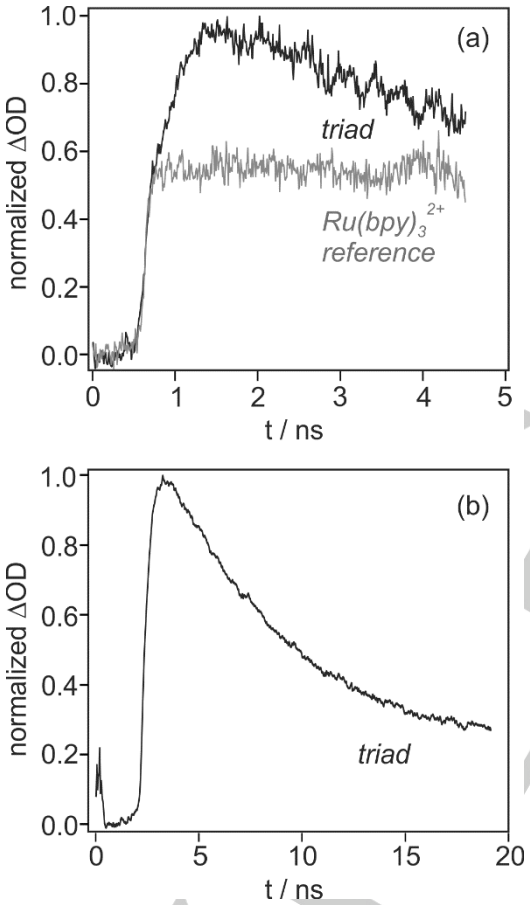

Figure 2. Temporal evolution of the emission-corrected transient absorption signal of **exTTF-PTZ-Ru(bpy)$_3^{2+}$** in CH_3CN integrated between 580 and 700 nm (black trace) and $[Ru(bpy)_3]^{2+}$ between 550 and 680 nm (gray trace) following excitation at 532 nm with laser pulses of ca. 30 ps duration. (b) Transient absorption of the solution from (a) in a longer time window. Laser excitation pulse occurs at t = 0.5 ns on the 5 ns time window and at t = 2 ns on the 20 ns time window.

After ca. 1.5 ns following the excitation pulse the transient absorption signal in Figure 2a begins to decay with a time constant of 6100 ps, reflecting the return of the molecular triad to its initial state via reverse thermal charge shift from $Ru(bpy)_3^+$ to $exTTF^{\bullet+}$. The longest observable time window on our ps transient absorption setup is 20 ns, and on that timescale the signal does not return completely to baseline (Figure 2b). On our ns flash photolysis setup, we observed a residual signal even after more than 500 ns (not shown), and we tentatively attribute this to a photodegradation product. Furthermore, we cannot exclude the population of a (long-lived) exTTT-based triplet excited state via energy transfer from ^{3}MLCT-excited $Ru(bpy)_3^{2+}$. Computational studies suggest that the lowest triplet excited states of TTF and PTZ lie higher in energy than the states considered here.[22]

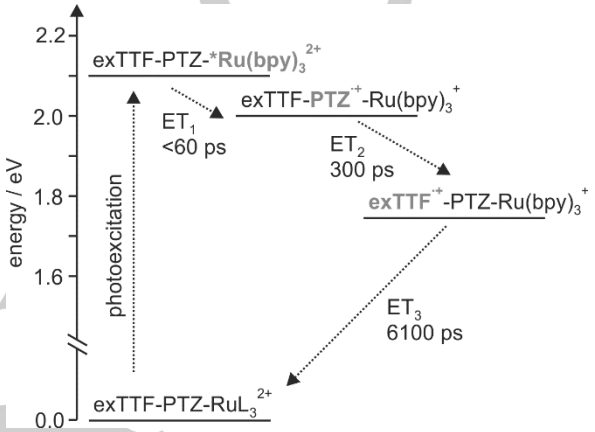

Scheme 3. Energy level diagram illustrating photoinduced charge-shift and thermal reverse charge-shift reactions in the triad from Scheme 2a. Energy levels were estimated based on the electrochemical data in Table 1.

In the following, we attempted to obtain evidence for charge accumulation on the exTTF unit of our triad by using methyl viologen (MV^{2+}) as an acceptor that can oxidize $Ru(bpy)_3^+$ bimolecularly following the initial rapid intramolecular electron transfer sequence observed above. Toward this end, the triad (2.5×10^{-5} M) was excited at 532 nm in presence of 50 mM MV^{2+} in de-aerated CH_3CN using pulses of ca. 10 ns duration. The resulting transient absorption spectrum (Figure 3a, solid trace) is dominated by spectral changes caused by the reduction of MV^{2+} to $MV^{\bullet+}$. This is evident from the dashed trace in Figure 3a, which is the difference spectrum obtained from electrochemical reduction of MV^{2+} to $MV^{\bullet+}$ (see Figure S7). To make transient absorption changes occurring from the triad more evident, the two spectra in Figure 3a were scaled to an identical ΔOD value at the $MV^{\bullet+}$ absorption maximum at 394 nm, and then the dashed trace was subtracted from the solid trace. The resulting difference spectrum (Figure 3b) exhibits a prominent absorption band centered around 650 nm, and based on the reference spectrum for $exTTF^{\bullet+}$ in Figure 3c (same spectrum as in Figures 1d and S4), this can be assigned to the one-electron oxidized terminal donor of the triad. Thus, the reaction sequence up to line (ii) in the right part of Scheme 1 has indeed occurred.

Given the rapid kinetics of intramolecular photoinduced electron transfer (300 ps, see above) and assuming diffusion-limited bimolecular electron transfer between $Ru(bpy)_3^+$ and 50 mM MV^{2+}

(1.9×10^{10} M^{-1} s^{-1} in CH_3CN at 25 °C, E^0 ($MV^{2+}/MV^{\bullet+}$ = -0.69 V vs. SCE),[23] secondary excitation of the regenerated photosensitizer, $Ru(bpy)_3^{2+}$, within the duration of the same 10-ns laser pulse might be possible. This could then induce the sequence of reactions (iii) – (vi) in Scheme 1, leading ultimately to $exTTF^{2+}$ (D_2^{2+} in Scheme 1). Indeed, the spectrum in Figure 3b exhibits a weak increase of absorbance at 490 nm, coincident with the wavelength at which the difference spectrum resulting from chemical oxidation of exTTF to $exTTF^{2+}$ with $SbCl_5$ has a maximum (Figure 3d). At shorter wavelengths, there are bleaches in the spectrum of Figure 3b resembling those in Figure 3d, but they merely reflect disappearance of neutral exTTF (Figure S2) and do not permit to distinguish between $exTTF^{\bullet+}$ and $exTTF^{2+}$.

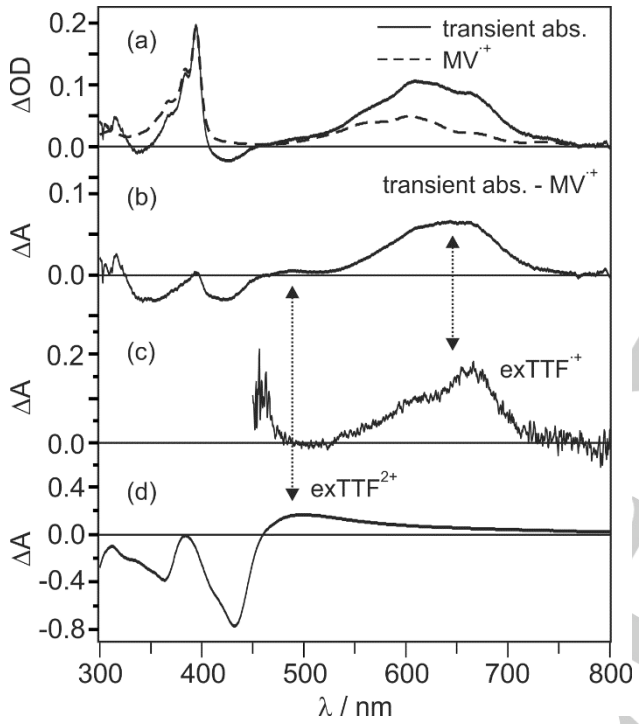

Figure 3. (a) Solid trace: Transient absorption spectrum recorded after 532 nm excitation (200 ns after excitation and time-integrated over 200 ns; laser pulse energy, 80 mJ) of **exTTF-PTZ-Ru(bpy)$_3^{2+}$** ($2.5\cdot10^{-5}$ M) in de-aerated CH_3CN (laser pulse duration ca. 10 ns) in presence of 50 mM $MV(PF_6)_2$. Dashed trace: Difference spectrum resulting from reduction of MV^{2+} to $MV^{\bullet+}$ (see Figure S7); scaled to the ΔOD value of the solid trace at 394 nm. (b) Difference spectrum generated by subtracting the dashed trace in (a) from the solid trace in (a). (c) Difference spectrum resulting from photochemical oxidation of **ref-exTTF** to **ref-exTTF$^{\bullet+}$** in DMF (same spectrum as in Figure 1d). (d) Difference spectrum resulting from chemical oxidation of the exTTF moiety of the triad to $exTTF^{2+}$ in DMF (see Figure S5).

Excitation power dependent measurements can often help to distinguish between photoproducts resulting from one- and two-photon excitation processes,[6a, 24] and therefore we recorded transient absorption spectra at two different laser pulse energies (15 and 80 mJ). However, shapes and relative signal intensities of the resulting spectra were completely identical.

The signal at 490 nm in Figure 3b is very weak, and in an attempt to find stronger evidence for hole accumulation on the exTTF unit of our triad, we performed additional two-color two-pulse flash photolysis experiments,[25] relying on a setup developed recently.[26] Specifically, an initial 532 nm laser pulse was followed by a secondary pulse exciting the same sample at 460 nm. At that wavelength near the ^{1}MLCT absorption maximum of the sensitizer, absorption by exTTF, $exTTF^{\bullet+}$ and $MV^{\bullet+}$ and is minimal (Figure S2 / S4 / S7). Thus, both pulses predominantly excited the $Ru(bpy)_3^{2+}$ sensitizer of the triad, and they both had a duration of ca. 10 ns but occurred with a delay of 500 ns. That delay time is ideal based on a two-pulse experiment monitoring kinetic transient absorption signals at the long-wavelength absorption band of $MV^{\bullet+}$ at 610 nm (Figure S8). We anticipated that this double excitation with a time delay of 500 ns would lead to more efficient two-fold oxidation of exTTF, assuming that the first pulse could induce the reaction sequences (i) – (ii) of Scheme 1 (right-hand side) whilst the second pulse could trigger reactions (iii) – (vi). Assuming the exclusive formation of the **exTTF$^{\bullet+}$-PTZ-Ru(bpy)$_3^{2+}$** / $MV^{\bullet+}$ charge-separated state with the first laser pulse, about 21 % of all triad molecules were converted to that state after primary excitation at 532 nm (estimated with the well-known molar absorption coefficient of $MV^{\bullet+}$ at 395 nm).[6c] However, despite the large fraction of primary photoproduct present, the transient absorption spectrum recorded after the second (blue) pulse (Figure S9a) is very similar to that obtained via single-pulse excitation (Figure 3a). Notably, the ratio between 490 and 650 nm absorbance changes is essentially identical in one- and two-pulse experiments (Figure S9b). Given this finding and the above-mentioned power-dependent studies, it seems unlikely that the weak feature at 490 nm arises from $exTTF^{2+}$, and it is more plausible that this feature is an artefact resulting from the imperfect correction of the spectra in Figure 3 and Figure S9.

Conclusions

Intramolecular photoinduced electron transfer in the triad from Scheme 2a occurs in stepwise fashion, involving oxidation of PTZ by ^{3}MLCT-excited $Ru(bpy)_3^{2+}$ on a sub-60-ps timescale, followed by oxidation of exTTF by $PTZ^{\bullet+}$ within 300 ps. The resulting photoproduct, **exTTF$^{\bullet+}$-PTZ-Ru(bpy)$_3^{+}$**, has a lifetime of 6100 ps in de-aerated CH_3CN at room temperature. In presence of excess methyl viologen $Ru(bpy)_3^{+}$ is rapidly oxidized, and there is clear evidence for **exTTF$^{\bullet+}$-PTZ-Ru(bpy)$_3^{2+}$** and $MV^{\bullet+}$. Weak transient absorption at 490 nm suggests the formation of **exTTF^{2+}-PTZ-Ru(bpy)$_3^{2+}$** resulting from twofold excitation of a given triad molecule within the same laser pulse and reaction along the sequence outlined in the right part of Scheme 1 (causing one-electron reduction of two MV^{2+} acceptor species). However, in a two-color two-pulse flash photolysis experiment the intensity of the signal at 490 nm does not increase relative to the absorbance at 660 nm caused by the $exTTF^{\bullet+}$ photoproduct resulting from single excitation and one-electron oxidation of the terminal donor, and excitation-power dependent experiments did not provide any evidence for $exTTF^{2+}$ either. Thus, there is likely no multi-electron transfer and charge accumulation in our triad.

Nevertheless, the strategy outlined in Scheme 1 appears promising, but more photochemically robust donor-donor-sensitizer triads will be desirable for further exploration of this concept. The combination with acceptors exhibiting less significant absorption changes upon reduction would be beneficial to more clearly detect the individual oxidation products, and to permit more straightforward discrimination between one- and two-electron oxidized donor species. Ultimately, it might even be desirable to extend this concept to fully integrated (all-covalent) donor-donor-sensitizer-acceptor-acceptor compounds, in which twofold oxidation of the terminal donor and twofold reduction of the terminal acceptor in the same molecular construct might become possible. To date, this has not been observed in molecular systems, and this would certainly represent a conceptual milestone on the way to emulating natural photosynthesis in artificial systems.

Experimental Section

^{1}H-NMR spectra were recorded on a Bruker Avance III NMR spectrometer with an operation frequency of 250 or 400 MHz at 298 K. Chemical shifts (δ) are given in ppm and were referenced on residual solvent peaks.[27] Coupling constants are reported in Hz. ESI mass spectra were measured on a Bruker Esquire 3000 plus ion-trap ESI-MS. High resolution ESI mass spectra were recorded by Mr Michael Pfeffer on a Bruker maXis 4G QTOF ESI spectrometer. Elemental analysis was performed by Ms Sylvie Mittelheisser on a Vario Micro Cube from Elementar.

UV-Vis absorption spectra were measured on a Varian Cary-5000 UV-Vis-NIR spectrometer. Cyclic voltammograms were recorded with a Versastat3-200 potentiostat from Princeton Applied Research. A three-electrode setup containing a glassy carbon working electrode, a silver wire counter electrode and an SCE reference electrode was used to measure the cyclic voltammograms. For spectro-electrochemical measurements, the Cary-5000 UV-Vis-NIR spectrometer and the Versastat3-200 potentiostat were used in combination. Here, a platinum net was used as working electrode, a platinum wire served as counter electrode and an SCE as reference electrode.

Nanosecond transient absorption spectra were recorded with an LP920-KS spectrometer from Edinburgh Instruments equipped with an Andor iCCD camera. Excitation at 532 nm occurred using pulsed second harmonic radiation with a Nd:YAG laser (Quantel Brilliant b, ca. 10 ns pulse width). Two-color two-pulse flash photolysis was performed on the same setup using an additional Quantel Brilliant laser equipped with an OPO from Opotek. Synchronization of the two lasers and the detection system was achieved as described previously.[26b] The output powers of both lasers were varied by the Q-switch delays and measured with a pyroelectric detector from Ophir. The beams of both lasers were sent through beam expanders (GBE02-A or GBE05-A, both from Thorlabs) to bring their diameters to either ~1.4 cm (blue laser; maximum laser intensity per area, 13 mJ/cm^2) or ~1.2 cm (green laser; maximum laser intensity per area, 70 mJ/cm^2). The beam expansion ensured completely homogeneous laser excitation in the whole detection volume (ca. 1.2 cm^3).

Emission-corrected picosecond transient absorption spectra were measured using a TRASS instrument from Hamamatsu and a mode-locked picosecond Nd:YVO_4/YAG laser (Ekspla model PL2251B-20-SH/TH/FH with PRETRIG option) as an excitation source. Briefly, the fundamental 1064 nm output was split into two pulse beams: one (pulse energy = 16 mJ) used to generate white light through excitation of a Xenon breakdown lamp, and the other directed through a second harmonic generation crystal to generate the 532 nm (1 mJ) excitation pulse. Samples were measured as de-aerated solutions with optical densities of 0.7 at the excitation wavelength.

Acknowledgments

Financial support by the Swiss National Science Foundation through grants number 200021_178760 and 206021_157687 (to OSW) and by the German National Academy of Sciences (to CK, postdoctoral fellowship LPDS 2017-11) is gratefully acknowledged.

Keywords: electron transfer • time-resolved spectroscopy • donor-acceptor systems • charge transfer • photochemistry

[1] a) L. Hammarström, *Acc. Chem. Res.* **2015**, *48*, 840-850; b) Y. Pellegrin, F. Odobel, *Coord. Chem. Rev.* **2011**, *255*, 2578-2593.

[2] a) R. Konduri, H. W. Ye, F. M. MacDonnell, S. Serroni, S. Campagna, K. Rajeshwar, *Angew. Chem. Int. Ed.* **2002**, *41*, 3185-3187; b) R. Konduri, N. R. de Tacconi, K. Rajeshwar, F. M. MacDonnell, *J. Am. Chem. Soc.* **2004**, *126*, 11621-11629; c) G. F. Manbeck, K. J. Brewer, *Coord. Chem. Rev.* **2013**, *257*, 1660-1675; d) K. Yamamoto, A. Call, K. Sakai, *Chem. Eur. J.* **2018**, *24*, 16620-16629; e) J. F. Lefebvre, J. Schindler, P. Traber, Y. Zhang, S. Kupfer, S. Gräfe, I. Baussanne, M. Demeunynck, J. M. Mouesca, S. Gambarelli, V. Artero, B. Dietzek, M. Chavarot-Kerlidou, *Chem. Sci.* **2018**, *9*, 4152-4159; f) L. Zedler, S. Kupfer, I. R. de Moraes, M. Wächtler, R. Beckert, M. Schmitt, J. Popp, S. Rau, B. Dietzek, *Chem.-Eur. J.* **2014**, *20*, 3793-3799; g) D. Polyansky, D. Cabelli, J. T. Muckerman, E. Fujita, T. Koizumi, T. Fukushima, T. Wada, K. Tanaka, *Angew. Chem. Int. Ed.* **2007**, *46*, 4169-4172; h) M. Skaisgirski, X. Guo, O. S. Wenger, *Inorg. Chem.* **2017**, *56*, 2432-2439; i) B. Matt, J. Fize, J. Moussa, H. Amouri, A. Pereira, V. Artero, G. Izzet, A. Proust, *Energy Environ. Sci.* **2013**, *6*, 1504-1508; j) A. G. Bonn, O. S. Wenger, *Chimia* **2015**, *69*, 17-21; k) A. G. Bonn, O. S. Wenger, *Phys. Chem. Chem. Phys.* **2015**, *17*, 24001-24010; l) J. N. Schrauben, R. Hayoun, C. N. Valdez, M. Braten, L. Fridley, J. M. Mayer, *Science* **2012**, *336*, 1298-1301.

[3] A. Pannwitz, O. S. Wenger, *Chem. Commun.* **2019**, *55*, 4004-4014.

[4] a) M. P. O'Neil, M. P. Niemczyk, W. A. Svec, D. Gosztola, G. L. Gaines, M. R. Wasielewski, *Science* **1992**, *257*, 63-65; b) H. Imahori, M. Hasegawa, S. Taniguchi, M. Aoki, T. Okada, Y. Sakata, *Chem. Lett.* **1998**, 721-722.

[5] a) S. Karlsson, J. Boixel, Y. Pellegrin, E. Blart, H. C. Becker, F. Odobel, L. Hammarström, *J. Am. Chem. Soc.* **2010**, *132*, 17977-17979; b) S. Karlsson, J. Boixel, Y. Pellegrin, E. Blart, H. C. Becker, F. Odobel, L. Hammarström, *Faraday Discuss.* **2012**, *155*, 233-252.

[6] a) M. Orazietti, M. Kuss-Petermann, P. Hamm, O. S. Wenger, *Angew. Chem. Int. Ed.* **2016**, *55*, 9407-9410; b) S. Mendes Marinho, M. H. Ha-Thi, V. T. Pham, A. Quaranta, T. Pino, C. Lefumeux, T. Chamaille, W. Leibl, A. Aukauloo, *Angew. Chem. Int. Ed.* **2017**, *56*, 15936-15940; c) T. T. Tran, M. H. Ha-Thi, T. Pino, A. Quaranta, C. Lefumeux, W. Leibl, A.

Aukauloo, *J. Phys. Chem. Lett.* **2018**, *9*, 1086-1091; d) M. Kuss-Petermann, O. S. Wenger, *Chem.-Eur. J.* **2017**, *23*, 10808-10814.

[7] M. Kuss-Petermann, M. Orazietti, M. Neuburger, P. Hamm, O. S. Wenger, *J. Am. Chem. Soc.* **2017**, *139*, 5225-5232.

[8] a) J. Nomrowski, O. S. Wenger, *J. Am. Chem. Soc.* **2018**, *140*, 5343-5346; b) J. Nomrowski, X. Guo, O. S. Wenger, *Chem.-Eur. J.* **2018**, *24*, 14084-14087.

[9] a) N. Dupont, Y. F. Ran, H. P. Jia, J. Grilj, J. Ding, S. X. Liu, S. Decurtins, A. Hauser, *Inorg. Chem.* **2011**, *50*, 3295-3303; b) C. Goze, C. Leiggener, S. X. Liu, L. Sanguinet, E. Levillain, A. Hauser, S. Decurtins, *ChemPhysChem.* **2007**, *8*, 1504-1512; c) C. Goze, N. Dupont, E. Beitler, C. Leiggener, H. Jia, P. Monbaron, S. X. Liu, A. Neels, A. Hauser, S. Decurtins, *Inorg. Chem.* **2008**, *47*, 11010-11017; d) C. Leiggener, N. Dupont, S. X. Liu, C. Goze, S. Decurtins, E. Breitler, A. Hauser, *Chimia* **2007**, *61*, 621-625; e) Y. S. Luo, M. Wächtler, K. Barthelmes, A. Winter, U. S. Schubert, B. Dietzek, *Phys. Chem. Chem. Phys.* **2018**, *20*, 11740-11748.

[10] a) D. Hanss, O. S. Wenger, *Eur. J. Inorg. Chem.* **2009**, 3778-3790; b) D. Hanss, O. S. Wenger, *Inorg. Chem.* **2009**, *48*, 671-680; c) R. J. Kumar, S. Karlsson, D. Streich, A. R. Jensen, M. Jäger, H. C. Becker, J. Bergquist, O. Johansson, L. Hammarström, *Chem.-Eur. J.* **2010**, *16*, 2830-2842; d) Y. S. Luo, J. H. Tran, M. Wächtler, M. Schulz, K. Barthelmes, A. Winter, S. Rau, U. S. Schubert, B. Dietzek, *Chem. Commun.* **2019**, *55*, 2273-2276; e) Y. S. Luo, K. Barthelmes, M. Wächtler, A. Winter, U. S. Schubert, B. Dietzek, *J. Phys. Chem. C* **2017**, *121*, 9220-9229; f) Y. S. Luo, K. Barthelmes, M. Wächtler, A. Winter, U. S. Schubert, B. Dietzek, *Chem. Eur. J.* **2017**, *23*, 4917-4922.

[11] a) J. Santos, B. M. Illescas, N. Martín, J. Adrio, J. C. Carretero, R. Viruela, E. Orti, F. Spanig, D. M. Guldi, *Chem. Eur. J.* **2011**, *17*, 2957-2964; b) N. Martín, L. Sánchez, D. M. Guldi, *Chem. Commun.* **2000**, 113-114; c) Y. Takano, M. A. Herranz, N. Martín, G. D. Rojas, D. M. Guldi, I. E. Kareev, S. H. Strauss, O. V. Boltalina, T. Tsuchiya, T. Akasaka, *Chem. Eur. J.* **2010**, *16*, 5343-5353.

[12] D. M. Guldi, L. Sanchez, N. Martín, *J. Phys. Chem. B* **2001**, *105*, 7139-7144.

[13] a) D. F. Perepichka, M. R. Bryce, I. F. Perepichka, S. B. Lyubchik, C. A. Christensen, N. Godbert, A. S. Batsanov, E. Levillain, E. J. L. McInnes, J. P. Zhao, *J. Am. Chem. Soc.* **2002**, *124*, 14227-14238; b) S. Wenger, P. A. Bouit, Q. L. Chen, J. Teuscher, D. Di Censo, R. Humphry-Baker, J. E. Moser, J. L. Delgado, N. Martin, S. M. Zakeeruddin, M. Grätzel, *J. Am. Chem. Soc.* **2010**, *132*, 5164-5169; c) Y. Yamashita, Y. Kobayashi, T. Miyashi, *Angew. Chem. Int. Ed.* **1989**, *28*, 1052-1053.

[14] a) B. M. Illescas, J. Santos, M. C. Diaz, N. Martín, C. M. Atienza, D. M. Guldi, *Eur. J. Org. Chem.* **2007**, 5027-5037; b) F. G. Brunetti, J. L. López, C. Atienza, N. Martín, *J. Mater. Chem.* **2012**, *22*, 4188-4205.

[15] C. K. Prier, D. A. Rankic, D. W. C. MacMillan, *Chem. Rev.* **2013**, *113*, 5322-5363.

[16] N. E. Gruhn, N. A. Macías-Ruvalcaba, D. H. Evans, *Langmuir* **2006**, *22*, 10683-10688.

[17] G. A. Heath, L. J. Yellowlees, P. S. Braterman, *J. Chem. Soc., Chem. Commun.* **1981**, 287-289.

[18] a) D. Hanss, O. S. Wenger, *Inorg. Chem.* **2008**, *47*, 9081-9084; b) H. C. Schmidt, X. W. Guo, P. U. Richard, M. Neuburger, C. G. Palivan, O. S. Wenger, *Angew. Chem. Int. Ed.* **2018**, *57*, 11688-11691.

[19] N. H. Damrauer, G. Cerullo, A. Yeh, T. R. Boussie, C. V. Shank, J. K. McCusker, *Science* **1997**, *275*, 54-57.

[20] J. Hankache, M. Niemi, H. Lemmetyinen, O. S. Wenger, *Inorg. Chem.* **2012**, *51*, 6333-6344.

[21] S. V. Rosokha, J. K. Kochi, *J. Am. Chem. Soc.* **2007**, *129*, 828-838.

[22] a) R. Pou-Amerigo, E. Orti, M. Merchan, M. Rubio, P. M. Viruela, *J. Phys. Chem. A* **2002**, *106*, 631-640; b) P. Borowicz, J. Herbich, A. Kapturkiewicz, R. Anulewicz-Ostrowska, J. Nowacki, G. Grampp, *Phys. Chem. Chem. Phys.* **2000**, *2*, 4275-4280.

[23] a) M. Montalti, A. Credi, L. Prodi, M. T. Gandolfi, *Handbook of Photochemistry*, CRC Taylor & Francis, Boca Raton, Florida, **2006**; b) M. Heyrovsky, *J. Chem. Soc., Chem. Commun.* **1987**, 1856-1857.

[24] A. Haefele, J. Blumhoff, R. S. Khnayzer, F. N. Castellano, *J. Phys. Chem. Lett.* **2012**, *3*, 299-303.

[25] M. H. Ha-Thi, V. T. Pham, T. Pino, V. Maslova, A. Quaranta, C. Lefumeux, W. Leibl, A. Aukauloo, *Photochem. Photobiol. Sci.* **2018**, *17*, 903-909.

[26] a) C. Kerzig, X. Guo, O. S. Wenger, *J. Am. Chem. Soc.* **2019**, *141*, 2122-2127; b) M. Kuss-Petermann, O. S. Wenger, *Helv. Chim. Acta* **2017**, *100*, e1600283.

[27] G. R. Fulmer, A. J. M. Miller, N. H. Sherden, H. E. Gottlieb, A. Nudelman, B. M. Stoltz, J. E. Bercaw, K. I. Goldberg, *Organometallics* **2010**, *29*, 2176-2179.

Entry for the Table of Contents

FULL PAPER

Photoinduced charge-shift reactions and the possibility of light-driven charge accumulation were explored in a molecular triad comprised of two donors and one photosensitizer.

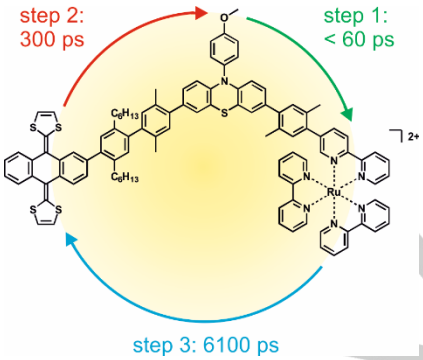

Charge accumulation

*Michael Skaisgirski, Christopher B. Larsen, Christoph Kerzig, and Oliver S. Wenger**

Page No. – Page No.

Stepwise photoinduced electron transfer in a tetrathiafulvalene-phenothiazine-ruthenium triad